MARTIN MARIETTA ENERGY SYSTEMS LIBRARIES
3 4456 0361240 0

CENTRAL RESEARCH LIBRARY
DOCUMENT COLLECTION

ORNL-2462
Physics and Mathematics

Cy. 4

GAMMA-RAY DOSE RATES RESULTING FROM NEUTRON CAPTURES IN AIR

F. L. Keller
C. D. Zerby
W. W. Dunn

CENTRAL RESEARCH LIBRARY
DOCUMENT COLLECTION
LIBRARY LOAN COPY
DO NOT TRANSFER TO ANOTHER PERSON
If you wish someone else to see this document, send in name with document and the library will arrange a loan.

OAK RIDGE NATIONAL LABORATORY
operated by
UNION CARBIDE CORPORATION
for the
U.S. ATOMIC ENERGY COMMISSION

Printed in USA. Price 125 cents. Available from the

Office of Technical Services
U. S. Department of Commerce
Washington 25, D. C.

LEGAL NOTICE

This report was prepared as an account of Government sponsored work. Neither the United States, nor the Commission, nor any person acting on behalf of the Commission:

A. Makes any warranty or representation, express or implied, with respect to the accuracy, completeness, or usefulness of the information contained in this report, or that the use of any information, apparatus, method, or process disclosed in this report may not infringe privately owned rights; or

B. Assumes any liabilities with respect to the use of, or for damages resulting from the use of any information, apparatus, method, or process disclosed in this report.

As used in the above, "person acting on behalf of the Commission" includes any employee or contractor of the Commission to the extent that such employee or contractor prepares, handles or distributes, or provides access to, any information pursuant to his employment or contract with the Commission.

ORNL-2462

Copy No. ___

Contract No. W-7405-eng-26

NEUTRON PHYSICS DIVISION

GAMMA-RAY DOSE RATES RESULTING FROM NEUTRON CAPTURES IN AIR

F. L. Keller C. D. Zerby
W. W. Dunn*

Date Issued
DEC 15 1958

OAK RIDGE NATIONAL LABORATORY
Oak Ridge, Tennessee
Operated by
UNION CARBIDE CORPORATION
for the
U.S. ATOMIC ENERGY COMMISSION

*On assignment from U. S. Air Force.

MARTIN MARIETTA ENERGY SYSTEMS LIBRARIES

3 4456 0361240 0

ABSTRACT

A Monte Carlo calculation of the gamma-ray fluxes and dose rates resulting from neutron captures in air was performed. For this calculation the source was assumed to be monoenergetic, and both the source and detector were assumed to be suspended in an infinite body of air. The neutron source was taken to be either a point isotropic or a line-beam source, and the dose rate and angular distribution of capture gamma rays at the detector were determined. For the point isotropic source and a 50-ft separation distance it was found that the dose rate varied with the neutron source energy approximately as $E^{-1/3}$. When curves for the various monoenergetic line-beam sources and a 65-ft separation distance were plotted as a function of the beam angle, they were relatively flat over the region from 30 to 180 deg, becoming flatter as the source energy increased.

TABLE OF CONTENTS

		Page No.
	Abstract	iii
	Introduction	1
I.	Details of the Calculation	2
	Assumed Composition of Air and Corresponding Cross Sections	3
	Geometry	3
	General Method of Calculation	5
	Determination of Constants for Gamma-Ray Dose Rate	7
	Test Calculations	14
	Calculation of Dose Rate from First Collisions	14
	Comparison with Results Obtained with Transport Equation	15
	Check on Statistics	18
II.	Results of Point Isotropic Neutron Sources	20
III.	Results for Line-Beam Neutron Sources	25
App. A.	Modification of Air-Scattering Code	29

INTRODUCTION

Very little quantitative work has been done previously on the problem of determining gamma-ray dose rates produced in air when low-energy neutrons are allowed to leave a source and are eventually captured in the air. The gamma rays which are produced by the radiative capture process in air are largely of rather high energy, ~ 5 to 10 Mev, and hence, are quite penetrating. In the majority of the shielding problems which occur in connection with the shielding of fission sources the gamma-ray dose rate which results from these air captures is negligible when compared with the dose rate produced by gamma rays which leave the source shield surface directly. However, situations may arise in which the source itself is heavily gamma-ray shielded, at least in the directions which are favorable for air scattering to the detector, but a large neutron leakage is allowed and perhaps auxiliary neutron shielding material is placed around the detector position. In many of these situations, the fact that the air-capture gamma rays are quite penetrating and often produced at positions which are very favorable for allowing the gamma rays to penetrate the auxiliary shield, makes it possible for the air-capture gamma rays to give a major contribution to the gamma-ray dose rate at the detector.

It is desirable to idealize the problem to that of determining the air-capture gamma-ray dose rate and angular distribution at a detector which is located an arbitrary distance from a point monoenergetic source of neutrons, where both the source and detector are considered to be embedded in an infinite sea of air. The calculation should include the contributions from captures which take place during the slowing-down process as well as the contributions from captures which occur during the diffusion at thermal energies.

If an attempt is made to solve this problem analytically for point isotropic sources by use of the standard age-diffusion equation, an immediate difficulty arises from the fact that, in many cases, a large contribution to the dose rates at the detector comes from neutrons which are captured at energies very close to the source energy. The age-diffusion results are known to break down in these cases. Even for the case of thermal diffusion alone

(i.e., the case where the neutrons are emitted from the source at thermal energy), for the separation distances of interest in these calculations, the contribution to the gamma-ray dose rate at the detector from the neutron flux distribution given by the nonasymptotic part of the solution to the transport equation is of the same order of magnitude as the contribution from the neutron flux distribution given by the asymptotic part (or diffusion equation result) of the solution to the transport equation. Hence, it appears that the most profitable approach to this problem is by means of the Monte Carlo technique. This technique has the benefit of being relatively easy to extend to cases of line-beam, or gun-barrel, neutron sources, in addition to being more rigorous.

This report presents the results of parameter studies for both point isotropic and line-beam neutron sources which were performed by the Monte Carlo technique. The processes and assumptions which were incorporated in the calculation are contained in Section I, together with the results of some test calculations and comparisons which were performed to evaluate the accuracy of the results. Section II presents the results of a parameter study from point isotropic sources and a detector located a distance of 50 ft from the source, and Section III gives the results for line-beam sources with the detectors at distances of 25 and 65 ft. A detailed description of the modifications which were made in an existing Monte Carlo code[1] to enable it to perform this calculation is given in Appendix A. The original code, together with a complete description of its operation and use, is given in the reference cited.

I. DETAILS OF THE CALCULATION

The Monte Carlo machine code which was used for this problem was a modification of the code used to calculate neutron air scattering. The original code has been described completely elsewhere;[1] therefore, the discussion here will be limited to a very brief description of the general features of the code as modified to perform the present problem. A detailed description of the exact code changes are given in Appendix A.

---

1. C. D. Zerby, "A Monte Carlo Calculation of Air-Scattered Neutrons," ORNL-2277 (April, 1957).

Assumed Composition of Air and Corresponding Cross Sections

The air was assumed to have a density of 0.001205 g/cc and to consist of nitrogen and oxygen in weight percentages of 76.5 and 23.5, respectively. The total cross sections for oxygen and nitrogen were taken from the graphs presented in BNL-325.[2] Analytic expressions, fit to the data, were used in the energy range of interest in the present problem. The total cross section was considered to be identical with the scattering cross section except for the absorption cross section of nitrogen. The absorption cross section for oxygen is extremely small and was neglected. The absorption cross section for nitrogen at 0.025 ev was taken to be 1.786 barns. This absorption cross section is due to the (n,p) and (n,γ) reactions. The (n,p) and (n,γ) reactions were taken to have cross sections of 1.706 barns and 0.086 barn, respectively, at 0.025 ev and were assumed to have a 1/v dependence. Theoretical investigations for nitrogen have indicated that "for almost all conceivable applications σ_γ can be taken as decreasing indefinitely as 1/v, but its true behavior can only be determined by fixing the existence and location of the negative energy levels."[3] The scattering probability for the neutrons was taken as isotropic in the center-of-mass system which is essentially exact for nitrogen and oxygen over the range of energies of interest in this problem. All of the results are normalized to one neutron per second leaving the source.

Geometry

The geometry of the source and detector are shown in Fig. 1. The source was taken to be either a point isotropic source of monoenergetic neutrons of energy E_o, or a point source which emitted a monoenergetic line beam of neutrons of energy E_o at an angle θ_o with respect to the source-detector axis. The detector was located a distance g from the source and the space about the detector was divided into a number of solid angles with their apexes at the detector point. The polar angle was divided into a number of equal angle intervals and the azimuthal angle was divided into a number of equal angle intervals. The meridian and parallels of latitude scribed on a sphere

2. D. J. Hughes and J. A. Harvey, "Neutron Cross Sections," BNL-325 (1955).
3. H. Lustig, H. Goldstein, and M. H. Kalos, "The Neutron Cross Sections of Nitrogen," NDA-86-1, p. 17 (1957).

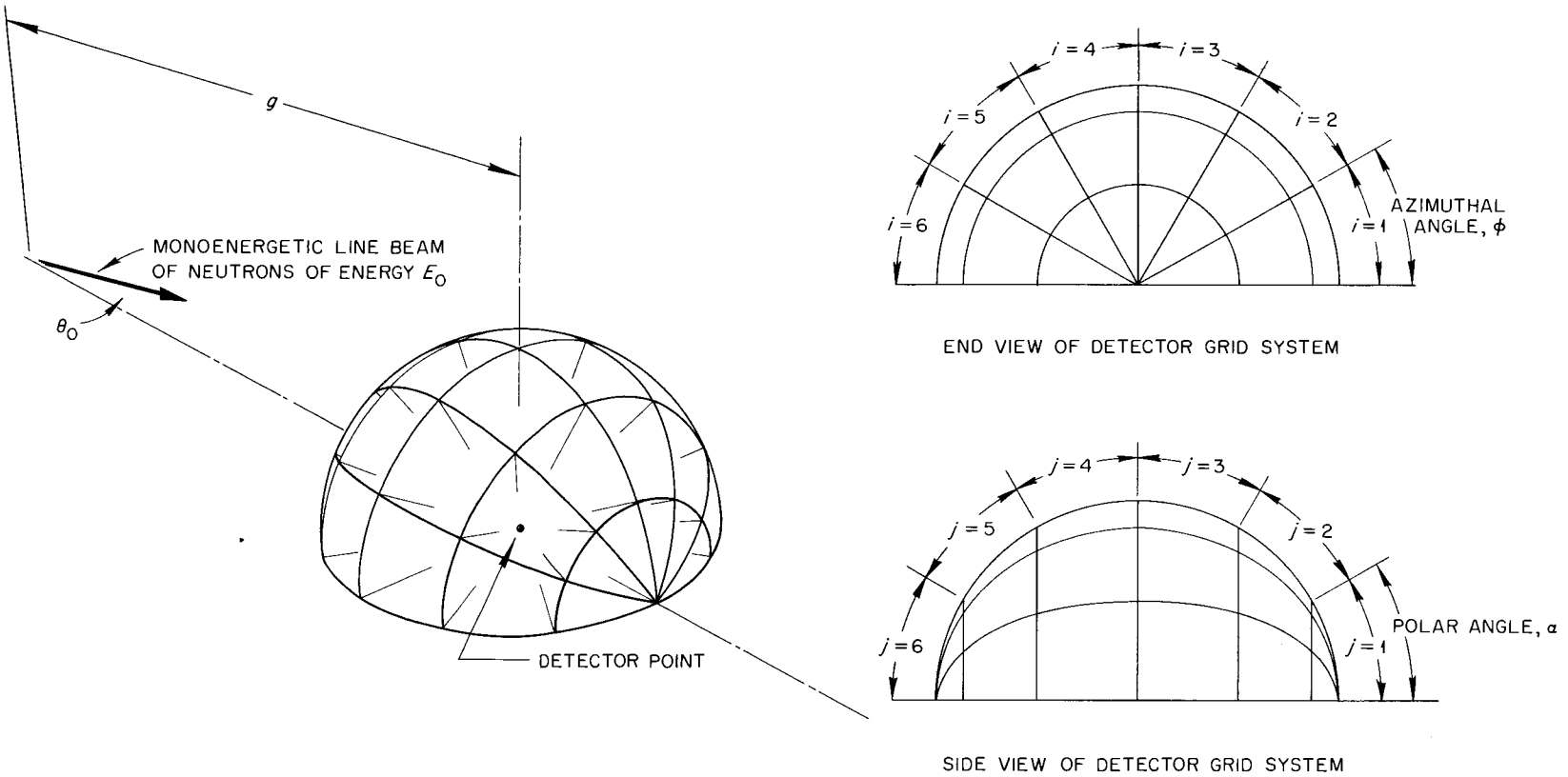

Fig. 1. Geometry Used in the Calculations of Air-Capture Gamma-Ray Dose Rates.

centered at the detector point established the intersection of the set of solid angles with the arbitrary sphere. Because of symmetry, the lower 2π space is just a reflection of the upper 2π space.

General Method of Calculation

The gamma-ray dose rate at the detector was obtained by an adaption of the method of statistical estimation. The histories of the neutrons were generated in exactly the same manner as described in the report on air scattering.[1] Each neutron carried with it a weight, W_ℓ, which is the probability that the particle will make the ℓth collision provided W_ℓ has a value of one at the start. That is,

$$W_{\ell+1} = W_\ell \frac{\Sigma_s(\vec{r}_\ell, E_\ell)}{\Sigma_t(\vec{r}_\ell, E_\ell)} \tag{1}$$

where Σ_s and Σ_t are the macroscopic scattering and total sections, respectively, at position $\vec{r}_\ell$ and energy E_ℓ (position and energy at the ℓth collision). At each collision a statistical estimate was made of the capture gamma-ray dose-rate contribution at the detector from that collision. The neutron was then allowed to scatter randomly and continue with its reduced weight. The capture gamma rays were assumed to be emitted isotropically from a capture event and the dose-rate contribution at the detector from the ℓth collision of a neutron was given by

$$AW_\ell \left[1 - \frac{\Sigma_s(\vec{r}_\ell, E_\ell)}{\Sigma_T(\vec{r}_\ell, E_\ell)}\right] \left(\frac{\Sigma_{n,\gamma}}{\Sigma_a}\right) \frac{e^{-br'_\ell}}{4\pi r'^2_\ell}$$

where

W_ℓ = neutron weight at the ℓth collision,

$\left[1 - \frac{\Sigma_s(\vec{r}_\ell, E_\ell)}{\Sigma_T(\vec{r}_\ell, E_\ell)}\right]$ = probability that the ℓth collision results in a capture,

$\left(\frac{\Sigma_{n,\gamma}}{\Sigma_a}\right)$ = probability that a capture collision will be radiative (a constant since both capture cross sections were assumed to vary as $1/v$),

r'_ℓ = scalar distance from the ℓth collision point to the detector,

b = average attenuation factor for the capture gamma-ray dose rate in air, which includes the effect of buildup,

A = constant which represents the average tissue dose rate (mr/hr) which would result if all the gamma rays from one neutron air capture per second were incident on a square centimeter of tissue.

This gamma-ray dose-rate contribution was stored in the appropriate solid angle interval at the detector under the assumption that all the gamma rays which gave the contribution entered in the interval which contained the radius vector from the detector to the collision point. The line-of-sight assumption for determining the angular distribution of the gamma-ray dose rate should be quite good in this case. The gamma-ray dose-rate contribution which entered in each solid angle interval was in turn stored with respect to the energy, at capture, of the neutron which gave rise to the contribution. This was accomplished by dividing the energy range from the neutron source energy to zero into an arbitrary number of equal intervals and entering each gamma-ray dose-rate contribution into the interval which contained the neutron energy at capture.

In this calculation the neutron was degraded in energy at each scattering by the standard relations for elastic collision until the neutron energy reached 0.025 ev. After the neutron energy was degraded to thermal (0.025 ev), the neutron was permitted to scatter and diffuse without further energy loss. A neutron history was terminated in one of two ways. First, if the neutron weight after the ℓth collision wereless than 1/600, i.e., if $W_{\ell+1} < 1/600$, then $W_{\ell+1}$ was set equal to zero and the history was terminated. This meant that a neutron with a source energy of 0.025 ev was permitted to make approximately 45 collisions before its history was terminated. Since the capture cross section decreases with increasing neutron energy, a neutron with higher initial energy would, of course, make many more collisions before the history was terminated by this criterion. Secondly, a neutron history was terminated if the ℓth collision occurred at a point sufficiently far from the detector

that $r_\ell' \Sigma_T(\vec{r}_\ell, E_\ell) \geq 32$. In this case $W_{\ell+1}$ was also set equal to zero and the history was terminated. This was because a neutron which makes a collision at a distance greater than 32 mfp from the detector has such a small probability of making a significant contribution to the dose rate on any of its succeeding collisions that it cannot appreciably affect the estimate of the total dose rate at the detector. For the neutron energies of interest in this problem 32 mfp corresponds to a distance of approximately 800 meters for an air density of 0.001205 g/cm^3. In each of the problems run the total neutron weight which was lost because of this condition was recorded and it is easily shown that the error introduced by this condition is, indeed, completely negligible.

Determination of Constants for Gamma-Ray Dose Rate

The constant A which appeared in Eq. 1 was defined as the average tissue dose rate (mr/hr) which would result if all the gamma rays from one neutron air capture per second were incident on one square centimeter of tissue. The spectrum of gamma rays from thermal-neutron capture by N^{14} has recently been remeasured by Bartholomew and Campion.[4] Table 1 gives the results of these measurements for the gamma rays with energies above 3 Mev which come from the decay of the excited N^{15} nucleus. A diagram of the energy levels of N^{15} and the decay scheme for the gamma rays observed is shown in Fig. 2. This diagram was used to estimate the number of gamma rays with energies less than 3 Mev which would be expected to result from the decay but which were not measured by Bartholomew and Campion.[4] Table 2 lists the approximate energy of each gamma ray, E_i, the average number of these gamma rays emitted per capture, N_i, and the flux-to-dose-rate conversion factor, C_i, for each gamma ray. It was assumed that the capture gamma-ray spectrum is independent of the energy at which the neutron is captured. Therefore, since the distribution in Table 2 gives the correct energy release per capture, i.e.,

$$\text{(2)} \qquad \text{Total energy per capture} = \sum_{i=1}^{22} E_i N_i = 10.83 \text{ Mev}$$

4. G. A. Bartholomew and P. J. Campion, Can. J. Physics 35, 1347 (Dec. 1957).

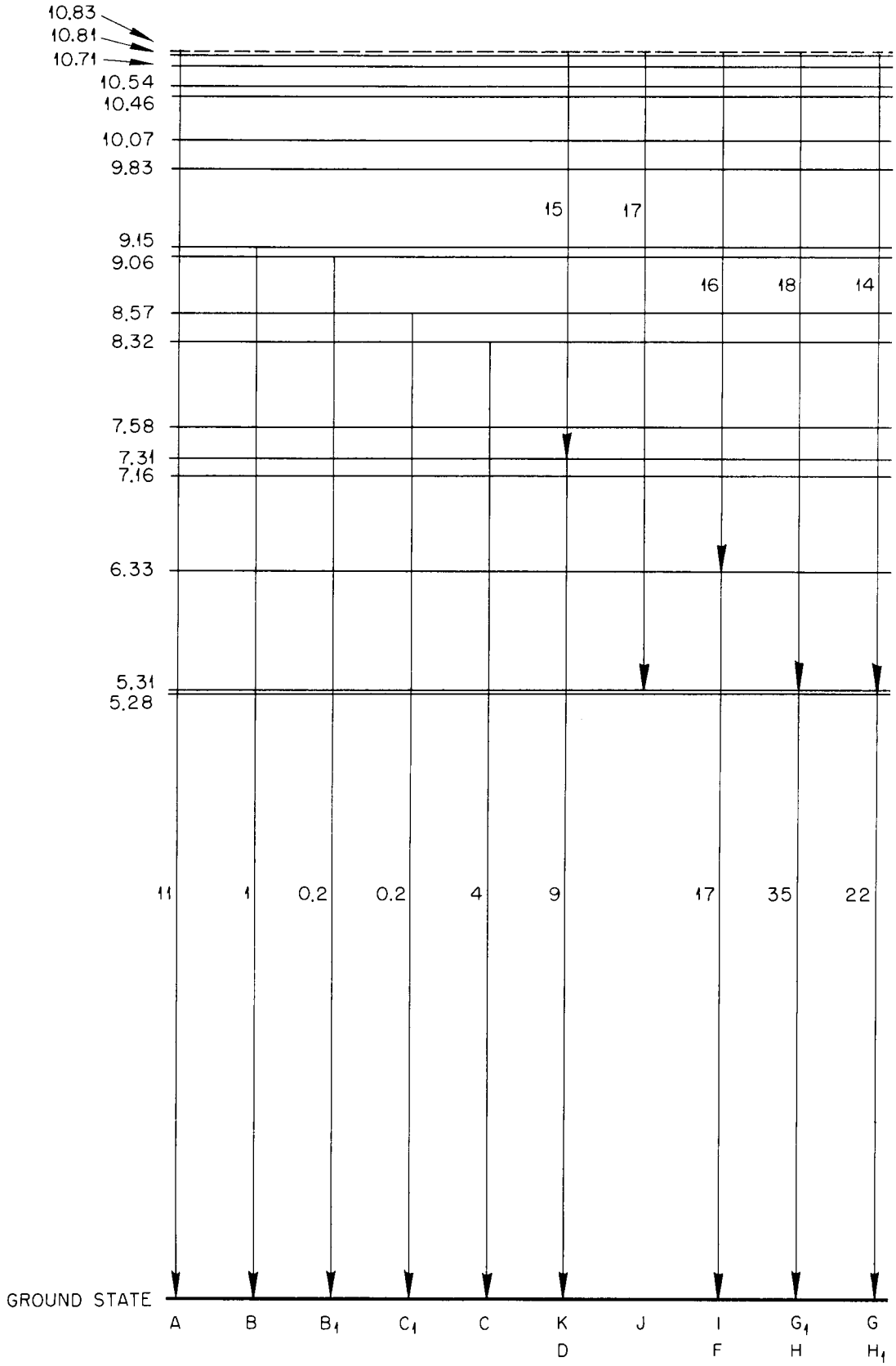

Fig. 2. Energy Level Diagram of N^{15} and Decay Scheme for Observed Capture Gamma Rays. (From Bartholomew and Campion, *Can. J. Phys.* 35, 1347 (1957).

Table 1. Observed Distribution of Gamma Rays from N^{14} Captures[a]

Gamma Ray[b]	Energy (Mev) Corrected for Recoil	No. of Gamma Rays per 100 Radiative Captures, Absolute Intensity
A	10.833 ± 0.008	11
	> 9.152[c]	Each ≤ 0.3
B	9.152 ± 0.010	1
B_1	9.02 ± 0.03	0.2
C_1	8.54 ± 0.04	0.2
C	8.313 ± 0.013	4
D	7.305 ± 0.012	9
E	7.57 ± 0.03[d]	0.7
	(7.164)	≤ 0.8
F	6.323 ± 0.008	17
G	5.559 ± 0.005	14 } 32[e]
G_1	5.530 ± 0.008	18 }
H	5.293 ± 0.007	35 } 57[e]
H_1	5.263 ± 0.010	22 }
I	4.497 ± 0.011	16
J	3.669 ± 0.016	17
K	3.520 ± 0.016	15
	(3.267)	≤ 6

a. Taken from Ref. 4.
b. Refer to Fig. 2.
c. All gamma rays between 9.152 and 10.833 Mev.
d. This radiation is ascribed to background. Its intensity represents an upper limit for the 7.57-Mev nitrogen transition.
e. Intensities of component gamma rays are tentative.

it follows that

$$A = \sum_{i=1}^{22} N_i C_i = 1.3 \times 10^{-2} \text{ mr}\cdot\text{hr}^{-1}/\text{capture}\cdot\text{sec}^{-1} \tag{3}$$

Next, it was necessary to determine a value for the constant b in Eq. 1. The variation of the total dose rate with distance for a point isotropic source of monoenergetic gamma rays may be expressed as

Table 2. Estimated Total Distribution of Gamma Rays from N^{14} Captures

i	E_i (Mev)	N_i (γ's/Capture)	C_i $\left(\frac{mr/hr}{\gamma's/cm^2 \cdot sec}\right)$	$N_i(E)C_i(E)$	$E_iN_i(E)$
1	10.83	1.1×10^{-1}	1.1×10^{-2}	1.21×10^{-3}	1.1913
2	9.15	1×10^{-2}	9.9×10^{-3}	9.9×10^{-5}	0.0915
3	9.03	2×10^{-3}	9.8×10^{-3}	1.96×10^{-5}	0.0181
4	8.54	2×10^{-3}	9.5×10^{-3}	1.90×10^{-5}	0.0171
5	8.31	4×10^{-2}	9.3×10^{-3}	3.72×10^{-4}	0.3324
6	7.30	9×10^{-2}	8.3×10^{-3}	7.47×10^{-4}	0.6570
7	7.16	8×10^{-3}	8.2×10^{-3}	6.56×10^{-5}	0.0573
8	6.32	1.7×10^{-1}	7.4×10^{-3}	1.26×10^{-3}	1.0744
9	5.56	1.4×10^{-1}	6.75×10^{-3}	9.45×10^{-4}	0.7784
10	5.53	1.8×10^{-1}	6.70×10^{-3}	1.21×10^{-3}	0.9954
11	5.29	3.5×10^{-1}	6.55×10^{-3}	2.29×10^{-3}	1.8515
12	5.26	2.2×10^{-1}	6.54×10^{-3}	1.44×10^{-3}	1.1572
13	4.50	1.6×10^{-1}	5.8×10^{-3}	9.28×10^{-4}	0.720
14	3.67	1.7×10^{-1}	4.95×10^{-3}	8.42×10^{-4}	0.6239
15	3.52	1.5×10^{-1}	4.8×10^{-3}	7.20×10^{-4}	0.5280
16	3.27	$\sim 6 \times 10^{-2}$	4.55×10^{-3}	2.73×10^{-4}	0.1962
17	2.52	4×10^{-2}	3.8×10^{-3}	1.52×10^{-4}	0.1008
18	2.29	2×10^{-3}	3.55×10^{-3}	7.10×10^{-6}	0.0046
19	2.00	6×10^{-2}	3.25×10^{-3}	1.95×10^{-4}	0.1200
20	1.86	1.62×10^{-1}	3.1×10^{-3}	5.02×10^{-4}	0.3013
21	1.80	2×10^{-3}	3.0×10^{-3}	6.0×10^{-6}	0.0036
22	1.68	1×10^{-2}	2.85×10^{-3}	2.85×10^{-5}	0.0168
				$\Sigma_i N_i C_i = 1.3 \times 10^{-2}$	$\Sigma_i E_i N_i = 10.8368$

$$\frac{e^{-\mu r}}{4\pi r^2} B_r(\mu r)$$

where μ is the total linear absorption coefficient at the source energy and B_r is the point isotropic dose buildup factor. The Compton scattering cross section

accounts for essentially the entire absorption coefficient, μ, in both air and water for gamma rays of the energies involved in the air-capture process. Therefore, the point isotropic dose buildup factors which have been published for gamma rays of various energies in water[5] may be assumed to apply also for air for corresponding numbers of mean free paths between the source and detector.

Figure 3 shows plots of $e^{-\mu r}B_r(\mu r)$ versus r for various energy gamma rays in air, as obtained from the water data. The heavy curve in Fig. 3 is the weighted dose attenuation curve for the spectrum given in Table 2. If this heavy curve were a straight line, then a value of b could obviously be obtained which would make the expression given on page 5 for the dose-rate contribution from each collision exactly correct. This, of course, is not the actual case; however, it can be seen from Fig. 3 that over the entire distance of interest (i.e., from 0 to 800 m) the heavy curve lies between the dashed curves given by $e^{-b_1 r}$ and $e^{-b_2 r}$, where b_1 and b_2 are 1.66×10^{-5} cm^{-1} and 2.32×10^{-5} cm^{-1}, respectively. Thus, the maximum error which can be introduced into the calculation by the choice of b may be determined by performing calculations with each of these extreme values. Variations in the value of this constant should, of course, have a greater effect on the results for cases with higher source energies since the higher source energies cause the captures to take place further from the detector and hence increase the importance of the exponential attenuation factor.

In order to estimate the possible error introduced by the choice of b, several sample calculations were performed. These calculations were designed to give gamma-ray dose rates at a distance of 50 ft from monoenergetic point isotropic sources of neutrons. Neutron source energies of 1, 100, and 1000 ev were used in conjunction with values of b of 0, 1.66×10^{-5} cm^{-1}, and 3.32×10^{-5} cm^{-1}. In each of the calculations for a particular source energy the same random numbers were used so that the individual neutron histories were exactly the same. Hence, the correlation between the results for different values of b at a given source energy should be very good. The results of these calculations are given in Table 3 and shown plotted in Fig. 4. The results for a particular source energy are seen to be relatively insensitive to the exact value of b used over the range

5. H. Goldstein and J. E. Wilkins, Jr., "Calculations of the Penetration of Gamma Rays," NYO-3075 (1954).

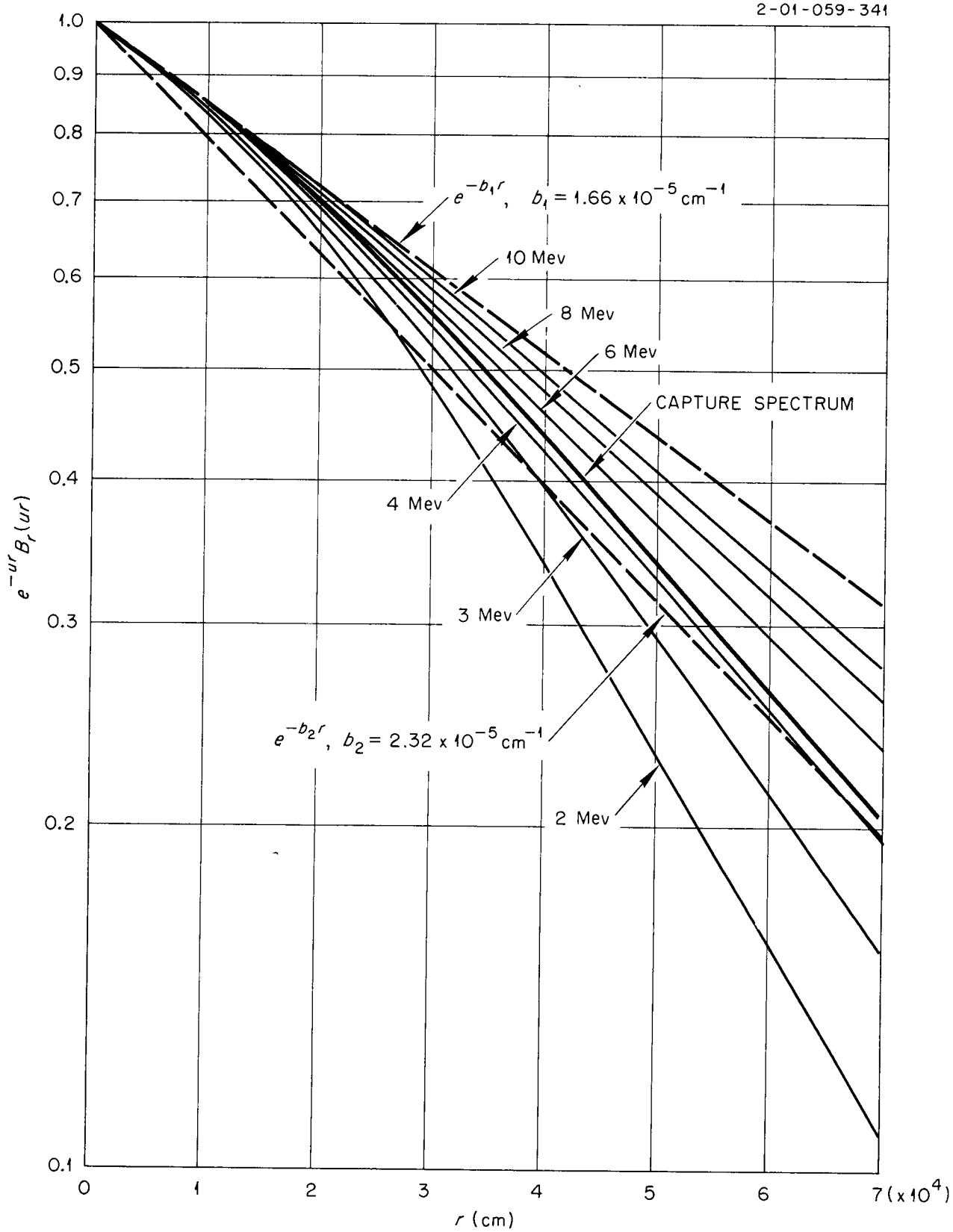

Fig. 3. Plots of $e^{-ur}B_r(ur)$ as a Function of r for Gamma Rays of Various Energies and for the Air-Capture Gamma-Ray Spectrum.

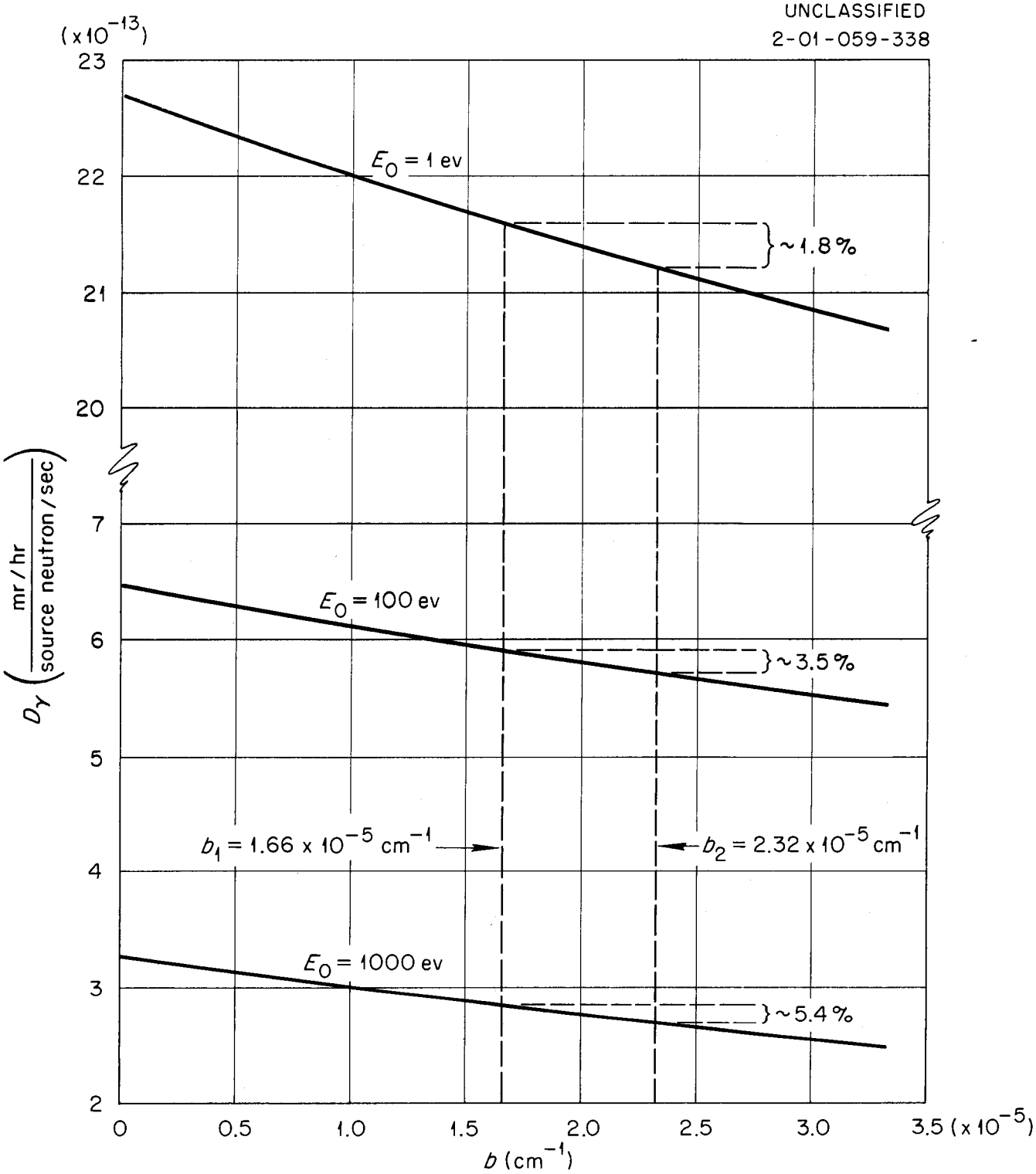

Fig. 4. Air-Capture Gamma-Ray Dose Rate at a Detector 50 ft from a Point Isotropic Neutron Source as a Function of b, the Attenuation Coefficient Assumed for Air, for Various Initial Neutron Energies E_0.

Table 3. The Effect of the Value of the Exponent b on Calculated Values of the Air-Capture Gamma-Ray Dose Rate

E_o (ev)	b (cm^{-1})	Gamma-Ray Dose Rate $\left(\frac{mr/hr}{source\ neutron/sec}\right)$
1.0	0	2.27×10^{-12}
	1.66×10^{-5}	2.16×10^{-12}
	3.32×10^{-5}	2.07×10^{-12}
100	0	6.47×10^{-13}
	1.66×10^{-5}	5.91×10^{-13}
	3.32×10^{-5}	5.45×10^{-13}
1000	0	3.27×10^{-13}
	1.66×10^{-5}	2.84×10^{-13}
	3.32×10^{-5}	2.50×10^{-13}

of interest. From this comparison, it is seen that even for a source energy of 1000 ev there is only a $\sim 5.5\%$ difference between the results expected for $b = 1.66 \times 10^{-5}\ cm^{-1}$ and $b = 2.32 \times 10^{-5}\ cm^{-1}$. This percentage difference becomes smaller, of course, as the source energy is decreased.

On the basis of the above comparison it was decided to use the value of $1.66 \times 10^{-5}\ cm^{-1}$ for b in the remainder of the calculations. This choice of b was influenced by several considerations. First, the dose rate does not appear to be extremely sensitive to the exact choice of b. Secondly, the curve of e^{-br} with b equal to $1.66 \times 10^{-5}\ cm^{-1}$ appears to fit the heavy curve of Fig. 3 very well at the closer separation distances, where most of the dose-rate contribution comes from. Finally, this choice of b should result in a conservative calculation in the sense that it gives an upper limit for the dose rate; however, it is an upper limit which should be very close to the correct answer.

Test Calculations

Calculation of Dose Rate from First Collisions

It was desirable to make several test calculations with the code to insure the fact that it was running properly. It was pointed out in the air scattering report[1] that when the point source emits a monodirectional beam of neutrons

the distances to the first-collision points are selected systematically. Therefore, this method is essentially a numerical integration for the gamma-ray dose rate from captures which take place on the first collision.

A test of the accuracy of the calculation for the gamma-ray dose-rate contribution to the detector from first collisions can easily be made for the particular condition where a monodirectional beam of neutrons is directed at 180 deg from the detector point. In this case, the analytic expression for the dose-rate contribution is given by

$$(4) \qquad D = \frac{A\Sigma_{n,\gamma}(E_o)}{4\pi} \int_g^{\infty} \frac{e^{-\Sigma_T(E_o)(x-g)} e^{-bx}}{x^2} \, dx$$

$$= \frac{A\Sigma_{n,\gamma}(E_o) e^{\Sigma_T g}}{4\pi g} E_2 \left[g(\Sigma_T + b) \right]$$

For the particular case where $g = 15$ m, $E_o = 0.025$ ev, and the air density is assumed to be 0.001205 g/cm^3, the analytic solution gives a value of 9.295928×10^{-13} mr·hr^{-1}/source neutron·sec^{-1}. The machine result for the same initial condition and 500 samples gives a value of 9.29599×10^{-13} mr·hr^{-1}/source neutron·sec^{-1}, or a per cent error of only ~ 0.0007.

Comparison with Results Obtained with Transport Equation

Next, it was desired to obtain an approximate check on the machine results for a case which involved many collisions. The only case which appeared to have the possibility of yielding a satisfactory analytical solution was that of a point isotropic source which emits monoenergetic 0.025-ev neutrons to scatter isotropically in the center-of-mass system without energy degradation. Since there is little difference between the Laboratory system and the center-of-mass system for a neutron scattering collision with either oxygen or nitrogen, it is possible to obtain a very good approximation to the neutron flux distribution in space for this case from the solution of the time-independent, monoenergetic transport equation for a point isotropic unit source located at the origin of an infinite, homogeneous, isotropically scattering medium. The transport equation for this case may be expressed as

(5) $$\vec{\Omega}\cdot\vec{\nabla}\phi(\vec{r},\vec{\Omega}) + \Sigma_T\phi(\vec{r},\vec{\Omega}) = \frac{\Sigma_s}{4\pi}\int\phi(\vec{r},\vec{\Omega})d\vec{\Omega} + \frac{\delta(\vec{r})}{4\pi}$$

where

$\vec{\Omega}$ = a unit vector,

$\phi(\vec{r},\vec{\Omega})$ = neutrons$\cdot$sec^{-1}/cm^2 per steradian about the direction at position $\vec{r}$,

$\frac{\delta(r)}{4\pi}$ = source term which represents a point isotropic unit source at the origin.

The total flux, $\Phi(r)$, or the total number of neutrons$\cdot$sec^{-1}/cm^2, at $\vec{r}$, is given by

(6) $$\Phi(\vec{r}) = \int\phi(\vec{r},\vec{\Omega})d\vec{\Omega}$$

The usual solution for $\Phi(\vec{r})$ consists of an asymptotic part which persists at large distances, $\Phi_{AS}(\vec{r})$, and a nonasymptotic part, $\Phi_{NONAS}(\vec{r})$. The asymptotic part, or diffusion approximation result, is given by

(7) $$\Phi_{AS}(\vec{r}) = \frac{K^2\beta e^{-Kr}}{4\pi\Sigma_a r}$$

where K satisfies

(8) $$\frac{\Sigma_s}{K}\tanh^{-1}\frac{K}{\Sigma_T} = 1$$

and

(9) $$\beta = 2\frac{\Sigma_a}{\Sigma_s}\left(\frac{\Sigma_T^2 - K^2}{K^2 - \Sigma_T\Sigma_a}\right)$$

The nonasymptotic part of the flux, $\Phi_{NONAS}(\vec{r})$, may be expressed as

(10) $$\Phi_{NONAS}(\vec{r}) = \frac{\epsilon(c,\Sigma_T r)e^{-\Sigma_T r}}{4\pi r^2}$$

where $c = \Sigma_s/\Sigma_T$ and $\epsilon(c,\Sigma_T r)$ is a function which has been tabulated by Case, deHoffman, and Placzek[6] for various values of c and $\Sigma_T r$.

6. K. M. Case, F. deHoffman, and G. Placzek, "Introduction to the Theory of Neutron Diffusion," p. 91, Los Alamos Scientific Laboratory (1953).

The air-capture gamma-ray dose rate at a detector located a distance g from the point source is therefore given by

$$D(g) = \frac{A\Sigma_{n,\gamma}}{4\pi} \int_{\text{All Space}} \Phi(r_1) \frac{e^{-br_2}}{r_2^2} dV \tag{11}$$

where r_1 and r_2 are distances from the field point to the source and detector, respectively. Equations 9 and 12 may be used to separate this total dose rate into contributions from the asymptotic and nonasymptotic parts of the flux expression. The contribution from the asymptotic part of the flux is given by

$$D_{AS}(g) = \frac{A\Sigma_{n,\gamma}K^2\beta}{16\pi^2\Sigma_a} \int_{\text{All Space}} \frac{e^{-Kr_1}e^{-br_2}}{r_1 r_2^2} dV \tag{12}$$

whereas the contribution from the nonasymptotic part is given by

$$D_{NONAS}(g) = \frac{A\Sigma_{n,\gamma}}{16\pi^2} \int_{\text{All Space}} \epsilon(C, \Sigma_T r_1) \frac{e^{-\Sigma_T r_1}e^{-br_2}}{r_1^2 r_2^2} dV \tag{13}$$

Equation 12 can be integrated directly to give

$$D_{AS}(g) = \frac{AK\beta}{8\pi g}\left(\frac{\Sigma_{n,\gamma}}{\Sigma_a}\right)\left\{e^{-Kg}\left\{\ln\left(\frac{K+b}{K-b}\right) + E_i\left[(K-b)g\right]\right\} + e^{Kg}\left\{E_1\left[(K+b)g\right]\right\}\right\} \tag{14}$$

where

$$E_i(x) = \int_{-\infty}^{x} \frac{e^y}{y} dy \text{ and } E_1(x) = \int_{x}^{\infty} \frac{e^{-y}}{y} dy \tag{15}$$

Equation 13 can be reduced to

$$(16) \quad D_{NONAS}(g) = \frac{A\Sigma_{n,\gamma}}{8\pi g}\left\{\int_0^\infty \frac{\epsilon(c,r)e^{-r}}{r}\left\{E_1\left[\delta|\alpha - r|\right] - E_1\left[\delta(\alpha + r)\right]\right\} dr\right\}$$

where $\alpha = \Sigma_T g$ and $\delta = b/\Sigma_T$; however, the actual evaluation must be performed numerically.

The evaluation of Eqs. 14 and 16 was performed, with the help of the tables of $\epsilon(c,r)$ given by Case et al., for a detector located 15 m from a point isotropic source of 0.025-ev neutrons. The values of the cross sections used were $\Sigma_T = 5.4402 \times 10^{-4}$ cm^{-1}, $\Sigma_s = 4.7364 \times 10^{-4}$ cm^{-1}, and $\Sigma_a = 7.038 \times 10^{-5}$ cm^{-1}, which resulted in $K = 3.215 \times 10^{-4}$ cm^{-1}, $\beta = 0.8797$, and $C = 0.8706$. The integrations yielded $D_{AS} = 5.024 \times 10^{-12}$ mr/hr and $D_{NONAS} = 2.118 \times 10^{-12}$ mr/hr or $D = 7.142 \times 10^{-12}$ mr/hr. The Monte Carlo result for 500 sample histories was $D = 6.4101 \times 10^{-12}$ mr/hr. Hence the results agree to within $\sim 10\%$ where it should be remembered that the two problems were not exactly the same. The Monte Carlo calculation took the scattering to be isotropic in the center-of-mass system, whereas the check calculation assumed the scattering to be isotropic in the laboratory system. This would be expected to lead to a slightly smaller value for the Monte Carlo result. In view of this fact, and the fact that a numerical integration which used interpolated values of $\epsilon(c,r)$ was required in the check calculation, the results are considered to be in satisfactory agreement. It is felt that all of the results presented in this report for total dose rates are probably good to within 10 to 20%.

It is interesting to notice that the dose-rate contribution from the nonasymptotic part of the flux expression accounted for 30% of the total dose rate in the above case.

Check on Statistics

Finally, a check was made of the variation in the Monte Carlo results as a function of the number of sample histories used for one particular problem. The case chosen was a line beam of 1000-ev neutrons emitted at an angle of 30 deg with respect to the source-detector axis. The detector was located 65 ft from the source and the air density was taken to be 0.001205 g/cm^3.

Table 4 gives the dose rate values obtained after 20, 50, 100, 250, 500, 750, and 1000 sample histories. The value obtained for the 1000-history case was taken as the correct value and the percentage errors of the results for smaller numbers of histories are included in Table 4. The variation in the

Table 4. Gamma-Ray Dose Rates 65 ft from 1000-ev Line-Beam Neutron Source and θ_0 = 30 deg for Various Numbers of Sample Histories

No. of Sample Histories	Gamma-Ray Dose Rate After Given Number of Histories $\left(\frac{\text{mr/hr}}{\text{source neutron}\cdot\text{sec}}\right)$	Per Cent Error Assuming 1000 History Case to be Correct
20	2.67×10^{-13}	1.87
50	2.87×10^{-13}	9
100	2.64×10^{-13}	0.75
250	2.49×10^{-13}	4.96
500	2.58×10^{-13}	1.5
700	2.58×10^{-13}	1.5
1000	2.62×10^{-13}	0

results appears to be relatively independent of the number of histories used and there appears to be no recognizable convergence to a unique answer as the number of histories is increased, at least for the number of histories used in this investigation. However, all of the results appear to agree to within $\sim$ 5 to 10%, which allows a fairly good estimate of the answer to be obtained with relatively few sample histories. This is typical of a Monte Carlo calculation of this type which employs the method of statistical estimation and allows the neutrons to make many collisions with only a small energy and weight decrease at each collision.

In the study which is reported in the remainder of this report, 500 sample histories were used in each of the problems run.

II. RESULTS FOR POINT ISOTROPIC NEUTRON SOURCES

A number of calculations were performed to give air-capture gamma-ray dose rates at a detector located at a distance of 50 ft from various mono-energetic, point isotropic neutron sources. For these calculations neutron source energies of 0.025, 0.1, 1.0, 100, and 10,000 ev were used. The density of air used in every problem was 0.001205 g/cc, which approximates sea level conditions. The results for the total gamma-ray dose rates from these calculations are given in Table 5. All of these results have been normalized to one neutron per second leaving the source. A plot of the total gamma-ray dose rate as a function of the neutron source energy is shown in Fig. 5. It may be noted from the plot that the total gamma-ray dose rate at the detector varies with the neutron source energy approximately as $E^{-1/3}$.

Table 5. Results of Monte Carlo Calculations of Capture Gamma-Ray Dose Rates at Detector Located 50 ft from Point Isotropic Neutron Sources

E_o (ev)	Gamma-Ray Dose Rate $\left(\frac{\text{mr/hr}}{\text{source neutron/sec}}\right)$
0.025	6.41×10^{-12}
0.1	4.22×10^{-12}
1.0	1.99×10^{-12}
10.0	9.54×10^{-13}
100.0	4.72×10^{-13}
10,000.0	1.15×10^{-13}

Plots of the angular distribution of the dose-rate contributions at the detector position are shown in Fig. 6. Since there is complete symmetry with respect to the azimuthal angle, the plots are given as dose rate per unit $\cos\alpha$ per source neutron per sec versus $\cos\alpha$, where α is the polar angle measured at the detector position. (α is defined so that a gamma ray produced on the section of the source-detector axis between the source and the detector, as well as on the other side of the source, enters the detector with $\cos\alpha = -1$.) These plots were obtained by drawing smooth

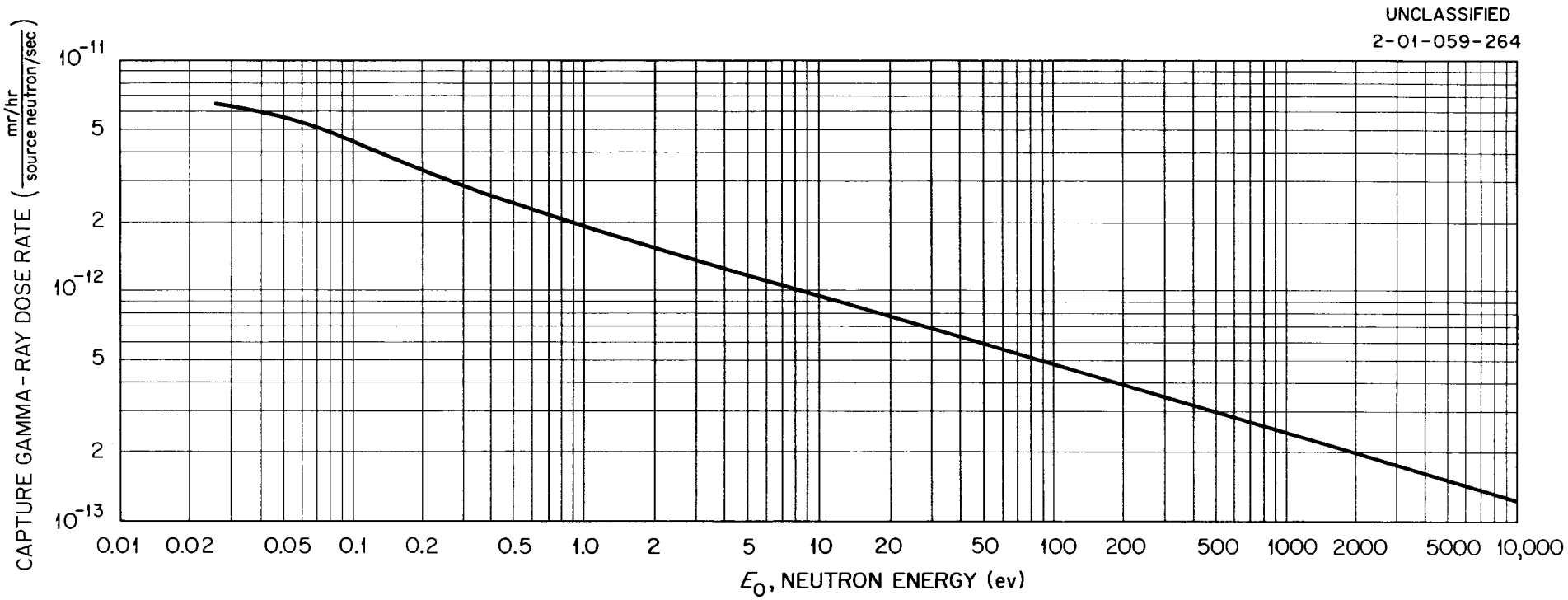

Fig. 5. Air-Capture Gamma-Ray Dose Rate at a Detector 50 ft from a Point, Isotropic Monoenergetic Neutron Source.

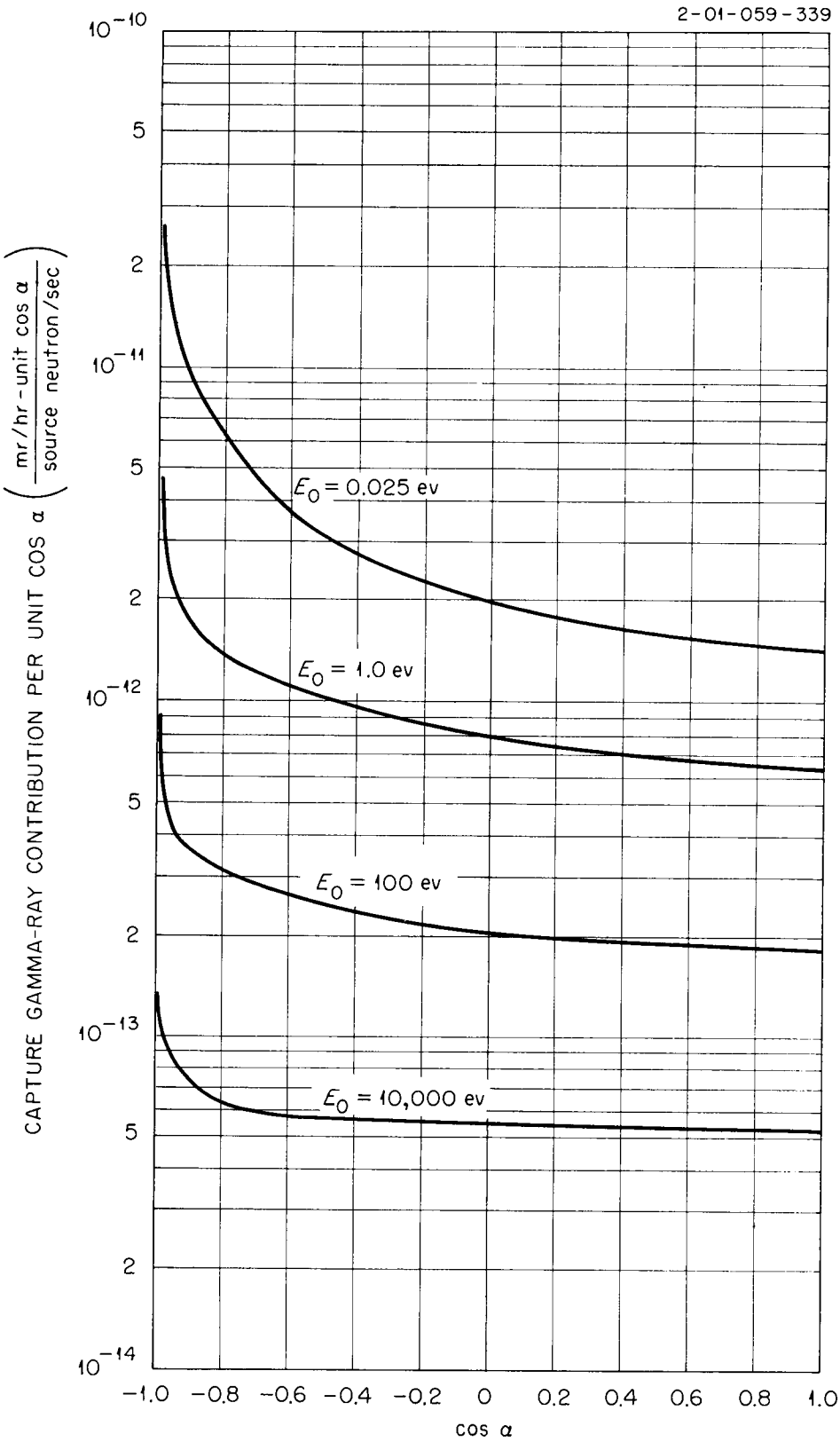

Fig. 6. Air-Capture Gamma-Ray Dose-Rate Contribution per Unit cos α at a Detector 50 ft from a Point Isotropic Neutron Source for Various Source Energies E_0.

curves through the histogram outputs from the machine calculations. As the neutron source energy is increased, more slowing down and diffusion results, on the average, before capture. This should cause the capture distribution to become more uniform over space, and, hence, lead to more uniform dose-rate angular distributions with increasing source neutron energies. This effect is seen in the curves of Fig. 6. If an angular distribution had been given to the scattered gamma rays which constitute the buildup portion of the dose-rate contribution from each collision, rather than assuming that all of the gamma rays enter along the radius vector from the collision point to the detector, then these dose-rate angular distribution curves would have been even flatter than those in the figure. However, this should be a rather small effect.

As was mentioned previously, each gamma-ray dose-rate contribution at the detector was also stored with respect to the energy, at capture, of the neutron which gave rise to the contribution. Figures 7 through 9 show histograms of the gamma-ray dose rate plotted as a function of the neutron capture energy for the cases considered in this study. From these figures it is seen that for relatively low neutron source energies, a large fraction of the total gamma-ray dose rate at the detector comes from neutrons which are captured at energies which are within a factor of α of the source energy, where $\alpha = \left[(A - 1)/(A + 1)\right]^2$ and A is the average mass number for air. This fact alone throws considerable doubt on calculations of capture gamma-ray dose rates which use the results of the standard age-diffusion equation to give the neutron flux because the age-diffusion results are known to be in error for neutron energies which are within a factor of α of the source energy. No curve is shown, of course, for the case where $E_o = 0.025$ ev since no energy degradation was allowed below this energy. It was pointed out in Section I, however, that in this case approximately 30% of the total dose-rate contribution at the detector comes from captures involving that part of the neutron flux given by the nonasymptotic part of the solution of the transport equation.

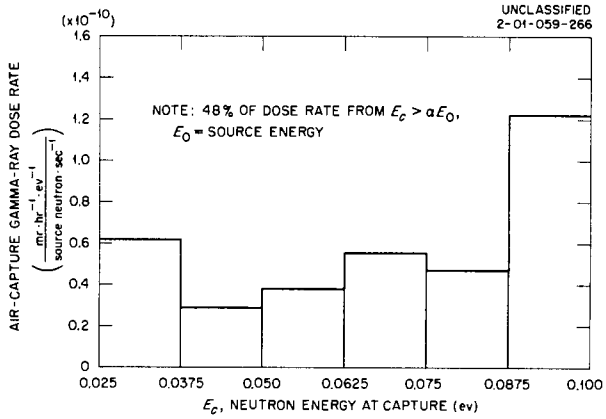

Fig. 7. Air-Capture Gamma-Ray Dose Rate 50 ft from a Point, Isotropic Neutron Source as a Function of E_c for E_o = 0.1 ev.

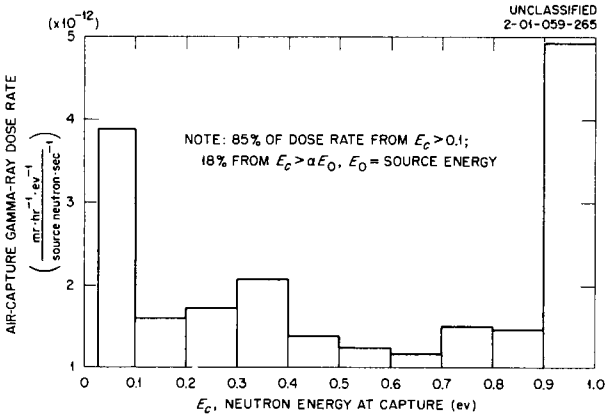

Fig. 8. Air-Capture Gamma-Ray Dose Rate 50 ft from a Point, Isotropic Neutron Source as a Function of E_c for E_o = 1.0 ev.

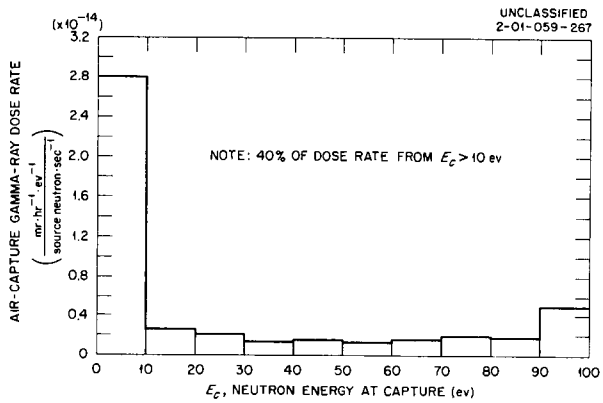

Fig. 9. Air-Capture Gamma-Ray Dose Rate 50 ft from a Point, Isotropic Neutron Source as a Function of E_c for E_o = 100 ev

III. RESULTS FOR LINE-BEAM NEUTRON SOURCES

For general applications it is convenient to obtain results for monodirectional, monoenergetic point sources, since the results can then be integrated to correspond to sources of arbitrary energy and angular distributions. Therefore, a parameter study was undertaken in which the line beams of neutrons with energies of 0.025, 0.1, 1, 10, 100, and 1,000 ev were emitted from a point source at various angles with respect to the source-detector axis and the air-capture gamma-ray dose rates at distances, g, of 25 and 65 ft from the source were determined. In all of the calculations the density of air was assumed to be 0.001205 g/cc, which approximates sea level conditions. It is possible, however, to transform the results to apply to different separation distances at other altitudes by the use of an appropriate transformation which has been derived elsewhere.[7] If D_{alt} and D_{sl} refer to dose rates at the desired altitude and at sea level, respectively, and ρ_{alt} and ρ_{sl} to the air density at the desired altitude and at sea level, respectively, then the transformation states that

$$D_{alt}\left(\frac{\rho_{sl}}{\rho_{alt}}\, g\right) = \frac{\rho_{alt}^2}{\rho_{sl}^2}\, D(g) \tag{17}$$

For example, the calculation for sea level conditions and g = 25 ft can be used to determine the dose rate for an altitude of 30,000 ft and an approximate separation distance of 65 ft.

The results for the total air-capture gamma-ray dose rates at the detector are shown plotted versus the angle of emission of the beam for the various monoenergetic sources in Figs. 10 and 11. It is interesting to note from these plots that the change in the capture gamma-ray dose rate with distance appears to be consistent with a 1/g dependence of the dose rate on the source-detector separation distance in this region for the case of 0.025-ev source neutrons. However, as the neutron energy is increased, the gamma-ray dose rate falls off less rapidly than 1/g in this region and

---

7. C. D. Zerby, "Radiation Flux Transformation as a Function of Density of an Infinite Medium with Anisotropic Point Sources," ORNL-2100 (1956).

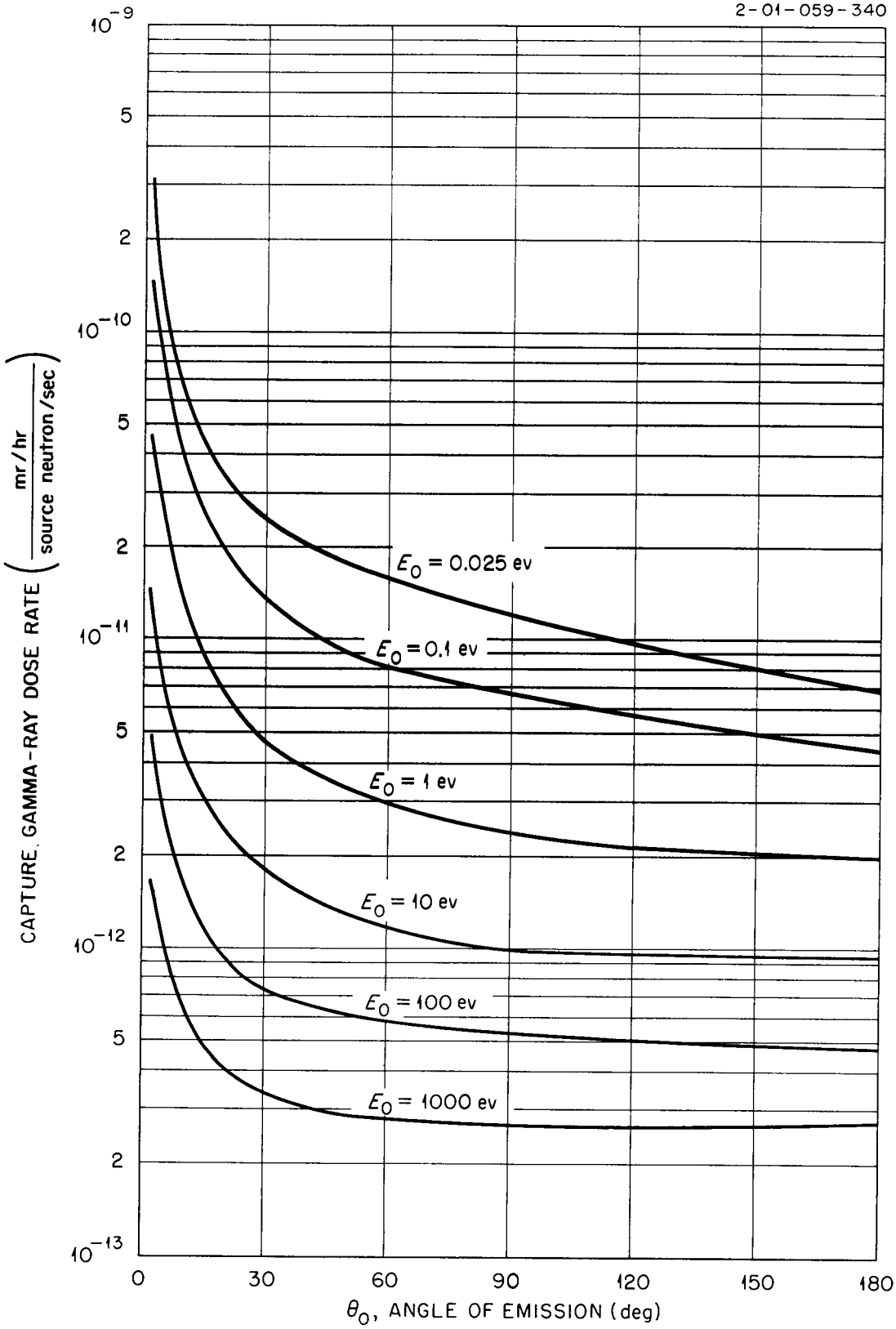

Fig. 10. Air-Capture Gamma-Ray Dose Rate at a Detector 25 ft from a Line Beam Neutron Source Emitted at Various Angles from the Source–Detector Axis.

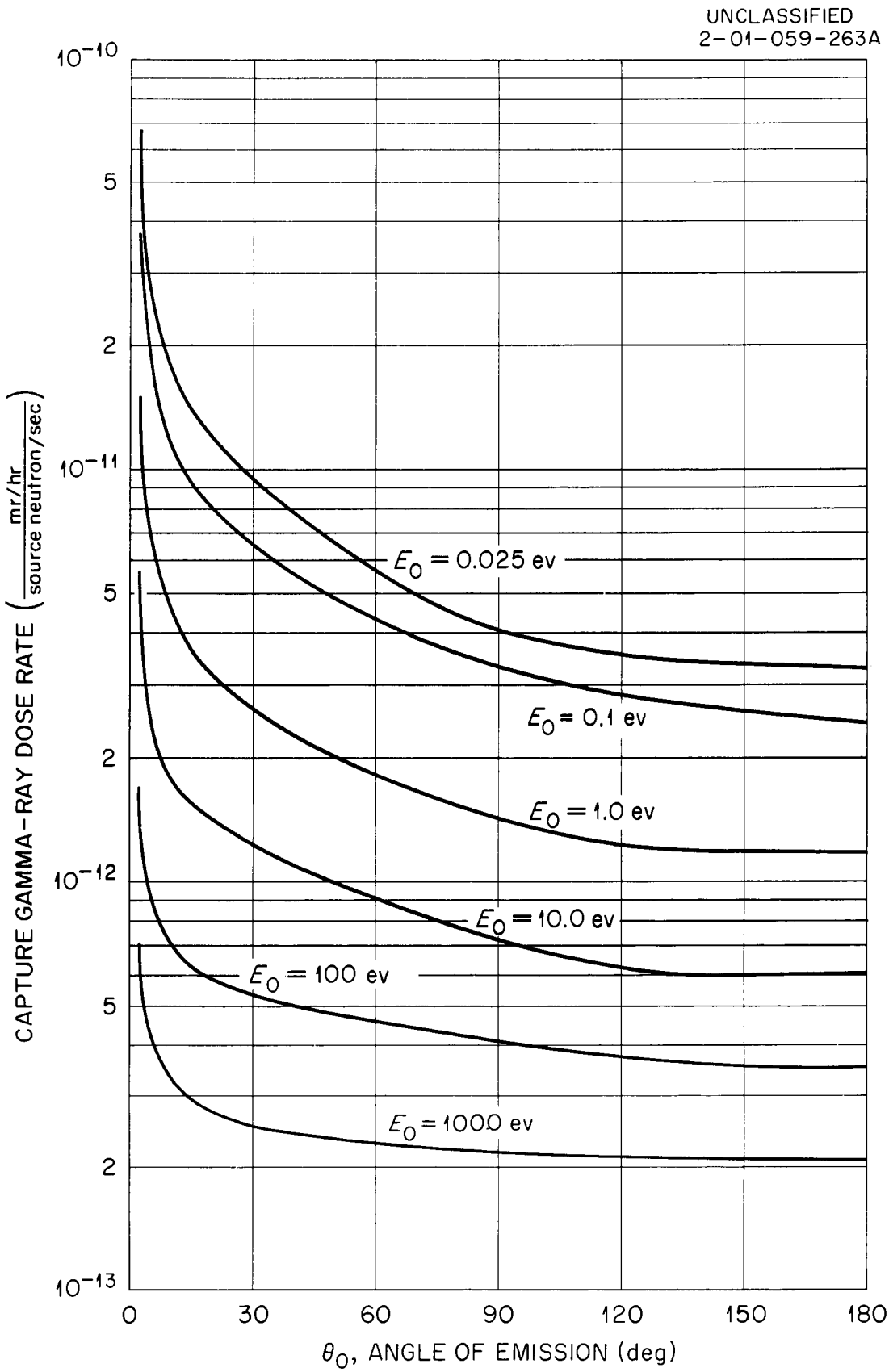

Fig. 11. Air-Capture Gamma-Ray Dose Rate at a Detector 65 ft from a Line Beam Neutron Source Emitted at Various Angles from the Source-Detector Axis.

it is seen from the plots that for a source-neutron energy of $\sim$1000 ev the dose rate changes by less than 20% in going from a separation distance of 25 ft to 65 ft. Hence, for a given air density, these calculations indicate that the gamma-ray dose-rate contributions from the higher-energy neutrons become more important relative to the contributions from the lower-energy neutrons as the source-detector separation distance is increased. On the other hand, by combining this result with Eq. 17 it is apparent that, for a fixed source-detector separation distance, the gamma-ray dose-rate contributions from the higher-energy neutrons become less important relative to the contributions from lower-energy neutrons as the altitude is increased (i.e., as the air density decreases).

Finally, a calculation was performed to estimate the maximum error which might be introduced if these point source results were applied to a source with finite dimensions. With this code it was possible to have the line beam of neutrons emerge from the surface of a black-absorbing sphere rather than from a point. In this case, a neutron history was immediately terminated if its path in space crossed the surface of the black sphere. Similarly, if the radius vector from any collision point to the detector passed through the black sphere, then the gamma-ray contribution from that collision was set equal to zero and the neutron was allowed to continue on. The maximum discrepancy between the results for the point source and the black-sphere source should obviously occur for the case of 0.025-ev neutrons emitted in a line beam at an angle of 180 deg with respect to the source-detector axis. Therefore, a problem was run to give the air-capture gamma-ray dose rate at 64 ft from a line beam of 0.025-ev neutrons emitted at θ_o = 180 deg from a black sphere with a diameter of 12 ft. The dose rate per source neutron per second for the black sphere case was 2.45×10^{-12} mr/hr. The result for the point source case was 3.52×10^{-12} mr/hr. Hence, even in this very extreme case the discrepancy was only $\sim$30%. In most practical cases the error introduced by applying the point source results to a finite source problem is probably within the statistical error of the point source results (i.e., $\sim$10 to 15%).

Appendix A

MODIFICATIONS OF AIR-SCATTERING CODE

This section of the report contains the information necessary to run the air-capture gamma-ray problem on the Oracle. The code used for this calculation is the "Neutron Air-Scattering Code" described in detail in Appendix B of ref. 1. For this calculation the following modifications should be made to the notes given in the reference:

Note I:

a. After item 5 the machine stops L-710. At this time have the operator correct the following addresses:

Address	Correct Word
65E →	60158 40012
160 →	43162 40800

b. Proceed by putting the code word for the name in the Q register as in item 6 and execute with S.O. 41710. Continue as before through step 11.

c. Step 12 requires a paper correction tape as follows:

Address	Correction		Address	Correction	
65E	25069	200AC	301	7F054	40000
2C9	412CA	00000	2EE	00132	0AEA1
2ED	4B2F2	432F6	2EF	00008	B403A
2F6	247BF	5F052	2F0	01400	00000
2F7	24367	5F054	302	24302	43043
2F8	242F8	43043	303	5F7F3	242F0
2F9	5F7F5	2635C	304	5F7BC	43305
2FA	14001	5F052	305	607BF	382EF
2FB	16000	7F054	306	1B019	41320
2FC	242FC	43043	325	5F7BC	40000
2FD	5F7F4	607ED	326	24326	43000
2FE	382EE	3A7F3	327	7BC27	BC7BC
2FF	40000	387E7	328	7BC27	BC7BC
300	5F052	16000	329	7BC27	BC7BC

Address	Correction		Address	Correction	
32A	FBC27	BC7BC	352	00000	43350
32B	2432B	43000	1A3	5F7F0	4B1B6
32C	7F527	F57F5	34C	247DF	5F7BF
32D	7BC17	F57F5	03D	1B001	5F7DC
32E	FF527	F47F4	041	1B001	5F7C5
32F	247F4	5F7BC	34D	41376	5F7E0
330	16000	777BC	28D	4134D	43299
331	43307	00000	34E	247BF	5F7DF
307	267BC	4B30A	34F	43299	24369
308	24308	43000	0B3	00000	000D5
309	FF327	F47F3	361	00000	000D5
30A	247DF	5F7F4	350	247DF	5F7BF
30B	41336	00000	351	412A3	00000
379	FF587	F6000	2AA	12006	4F29B
37A	4337B	00000	2AF	207F4	12006
356	227E0	4B30C	2B5	12006	4F29B
30C	247EC	14009	2C1	247F3	1C019
30D	227ED	4B28B	2C4	1C019	3B7E8
30E	4129E	00000	2C6	247F5	1C019
0AA	01000	00000	2E9	1C018	3B7E8
37B	412A3	00000	FFF		

Note X:

a. The digit A_1 which appears in input parameter P-0 can only have values 0 or 2.

b. Input parameter P-4 is changed from $E \cdot 10^{-2}$ to E with new range 0.025 ev $\leq E \leq$ 0.99 Mev.

c. Input parameter P-5 is changed from $E_c \cdot 10^{-2}$ to E_c with new range $0 \leq E_c \leq 0.99$ Mev.

d. Input parameter P-11 must be zero.

Note XI:

a. The output will now consist of one set of data that will be termed the flux output; however, the data designated as D_{jik} will be interpreted as:

D_{jik} = capture gamma-ray dose rate, mr/hr, at the detector point normalized to one source neutron per second in the kth energy interval of the neutron creating the gamma rays and in the ith azimuthal angle interval of the jth polar angle interval of the detector.

Note that these quantities are not normalized per unit energy per unit solid angle.

b. The following M values of the output will be altered to have the meanings given below:

M-5 Total gamma-ray dose rate ($mr \cdot hr^{-1}$/source neutron$\cdot sec^{-1}$) (f.p.)

M-6 Standard deviation on M-5 (f.p.)

M-7 Blank

M-8 Blank

M-13 - M-20 Blank

INTERNAL DISTRIBUTION

1. C. E. Center
2. Biology Library
3. Health Physics Library
4-5. Central Research Library
6. Reactor Experimental Engineering Library
7-40. Laboratory Records Department
41. Laboratory Records, ORNL R.C.
42. A. M. Weinberg
43. L. B. Emlet (K-25)
44. J. P. Murray (Y-12)
45. J. A. Swartout
46. E. H. Taylor
47. E. D. Shipley
48. A. H. Snell
49. E. P. Blizard
50. M. L. Nelson
51. W. H. Jordan
52. G. E. Boyd
53. R. A. Charpie
54. S. C. Lind
55. F. L. Culler
56. A. Hollaender
57. J. H. Frye, Jr.
58. M. T. Kelley
59. J. L. Fowler
60. R. S. Livingston
61. K. Z. Morgan
62. T. A. Lincoln
63. A. S. Householder
64. C. P. Keim
65. C. S. Harrill
66. C. E. Winters
67. D. S. Billington
68. H. E. Seagren
69. D. Phillips
70. A. J. Miller
71. R. R. Dickison
72. M. J. Skinner
73. J. A. Harvey
74. A. Simon
75. F. C. Maienschein
76. C. E. Clifford
77. A. D. Callihan
78. R. R. Coveyou
79. W. Zobel
80. F. L. Keller
81. D. K. Trubey
82. C. D. Zerby
83. S. K. Penny
84. R. W. Peelle
85. L. Jung
86. E. G. Silver
87. G. deSaussure
88. G. T. Chapman
89. F. L. Friedman (consultant)
90. H. Goldstein (consultant)
91. H. Hurwitz, Jr. (consultant)
92. L. W. Nordheim (consultant)
93. R. R. Wilson (consultant)
94. ORNL-Y-12 Technical Library, Document Reference Section

EXTERNAL DISTRIBUTION

95-96. C. E. Chapman, Dr. Donaldson, Convair - General Dynamics
97. K. L. Rooney, Curtiss-Wright Corporation
98-103. F. A. Aschenbrenner, J. MacDonald, W. E. Edwards, J. Carver, R. H. Clark, L. S. Burns, General Electric Company (ANPD)
104. R. V. Meghreblian, Jet Propulsion Laboratory
105-106. J. C. Flack, F. N. Watson, AFPR, Lockheed, Marietta
107. I. M. Karp, National Advisory Committee for Aeronautics, Cleveland
108-109. C. R. Fink, J. Weddell, The Martin Company, Baltimore
110-111. T. K. Krueger; L. A. Bowman, WCLJX; Wright Air Development Center
112-715. Given distribution as shown in TID-4500 (13th ed., Rev.) under Physics and Mathematics (75 copies OTS)